Showcasing research from the group of Dr Shuxiang Yang at Zhejiang Lab and Prof. Peng Zhang at Xi'An Jiaotong University, China

Discovery of superconductivity in technetium borides at moderate pressures

This research conducted thorough investigations on the superconductivity, mechanical properties and phase stability of the technetium–boron binary system. Five unprecedented superconducting technetium–borides were discovered at moderate or even ambient pressure, representing a fresh group in the family of superconducting metal–borides. The 4d-electrons of technetium play a dominant role for the electron–phonon coupling in these superconducting technetium–borides, in contrast with MgB_2. The various structures and stoichiometries of these superconducting technetium–borides suggest rich possibilities in looking for other superconducting transition-metal borides.

ROYAL SOCIETY OF CHEMISTRY

rsc.li/pccp

Registered charity number: 207890

PCCP Owner Societies

Check for updates

Discovery of superconductivity in technetium borides at moderate pressures†

Xiangru Tao,‡[a] Aiqin Yang,‡[a] Yundi Quan,[a] Biao Wan,[b] Shuxiang Yang*[c] and Peng Zhang ⓘ *[a]

Advances in theoretical calculations have boosted the search for high-temperature superconductors, such as sulfur hydrides and rare-earth polyhydrides. However, the required extremely high pressures for stabilizing these superconductors has handicapped further implementation. Based upon thorough structural searches, we identified a series of unprecedented superconducting technetium borides at moderate pressures, including TcB ($P6_3/mmc$) with a superconducting transition temperature of $T_c = 20.2$ K at ambient pressure and TcB$_2$ ($P6/mmm$) with $T_c = 23.1$ K at 20 GPa. Superconductivity in these technetium borides mainly originates from the coupling between the low-frequency vibrations of technetium atoms and the dominant technetium-4d electrons at the Fermi level. Our work therefore presents a fresh group in the family of superconducting borides, whose diversified crystal structures suggest rich possibilities in the discovery of other superconducting transition-metal borides.

1 Introduction

The discovery of superconductivity in mercury[1] motivated a century-long race for higher-temperature superconductors. Owing to the progress in theoretical calculations,[2–5] numerous high-temperature superconducting hydrides have been discovered in the past decade, including H$_3$S ($T_c \approx 191$–204 K at 200 GPa)[6,7] and LaH$_{10}$ ($T_c \approx 274$–286 K at 210 GPa) with record-high superconducting transition temperatures.[8–11] However, the stable presence of these superconducting hydrides requires very high pressures, which largely limits their potential implementations.[12–14]

Among all Bardeen–Cooper–Schrieffer (BCS) superconductors, borides represent a unique category with superconductivity at relatively low pressures. MgB$_2$ has the highest superconducting transition temperature, $T_c = 39$ K, among all BCS-type superconductors at ambient pressure.[15] At present, the discovered bulk superconducting borides with the same stoichiometry as MgB$_2$ include CaB$_2$ ($T_c \sim 50$ K[16] or 9.4–28.6 K[17] at ambient pressure, theory), NbB$_2$ ($T_c \sim 9.2$ K at ambient pressure, experiment[18–20]),

OsB$_2$ ($T_c = 2.1$ K at ambient pressure, experiment[21]), RuB$_2$ ($T_c = 1.6$ K at ambient pressure, experiment[21]), ScB$_2$ ($T_c = 1.5$ K at ambient pressure, experiment[22]), WB$_2$ (maximum $T_c = 15$ K at 100 GPa, experiment[23]), ZrB$_2$ ($T_c = 5.5$ K at ambient pressure, experiment[24]), SiB$_2$ ($T_c = 21$ K at ambient pressure, theory[25]) and MoB$_2$ ($T_c = 32$ K at 100 GPa, experiment[26]). Superconducting borides with other stoichiometries include X$_7$B$_3$ (X = Re and Ru with $T_c = 3.3$ and 2.6 K, respectively, at ambient pressure, experiment[27,28]), Re$_3$B ($T_c = 4.8$ K at ambient pressure, experiment[28]), X$_2$B (X = Mo, Re, Ta and W with $T_c = 5.1$, 2.8, 3.1 and 3.2 K, respectively, at ambient pressure, experiment[27]), XB (X = Hf, Nb, Mo, Ta and Zr with $T_c = 3.1$, 8.3, 0.5, 4.0 and 2.8–3.4 K, respectively, at ambient pressure, experiment[27]), FeB$_4$ ($T_c = 2.9$ K at ambient pressure, theory and experiment[29,30]), XB$_5$ (X = Na, K, Rb, Ca, Sr, Ba, Sc and Y with $T_c = 17.5$, 14.7, 18.6, 6.6, 6.8, 16.3, 14.2 and 12.3 K, respectively, at ambient pressure, theory[31]), BeB$_6$ ($T_c = 24$ K at 4 GPa, theory[32]), CB$_6$ ($T_c = 12.5$ K at ambient pressure, theory[33]), MgB$_6$ ($T_c = 9.5$ K at 32.6 GPa, theory[34]), ScB$_6$ (in $P2_1/m$-, $C2/m$- and $Cmcm$-structure with $T_c = 5.8$ K at ambient pressure, 2.2 K at 500 GPa, and 2.6 K at 800 GPa, respectively, theory[35]), XB$_6$ (X = Nb, La, Th and Y with $T_c = 3.0$, 5.7, 0.74 and 7.1 K, respectively, at ambient pressure, experiment[27]), XB$_7$ (X = Li, Na, K, Mg, Ca and Sr with $T_c = 21.6$, 18.3, 26.2, 29.3, 7.7 and 12.7 K, respectively, at ambient pressure, theory[36]), RbB$_6$ and RbB$_8$ ($T_c = 7.3$–11.6 K and 4.8–7.5 K at ambient pressure, respectively, theory[37]), YB$_6$ ($T_c = 7.2$ K at ambient pressure, experiment[38]), LaB$_8$ ($T_c = 14$ K[39] or 20 K[40] at ambient pressure, theory), XB$_{12}$ (X = Nb, La, Th, Y and Zr with $T_c = 3.0$, 5.7, 0.74, 7.1 and 5.8 K, respectively, at ambient pressure, experiment[27,41–43]), ternary borides like SrB$_3$C$_3$ ($T_c = 22$ K at 23 GPa, theory and

[a] *MOE Key Laboratory for Non-equilibrium Synthesis and Modulation of Condensed Matter, Shaanxi Province Key Laboratory of Advanced Functional Materials and Mesoscopic Physics, School of Physics, Xi'an Jiaotong University, Xi'an, Shaanxi, 710049, P.R. China. E-mail: zpantz@mail.xjtu.edu.cn*

[b] *Key Laboratory of Material Physics of Ministry of Education, School of Physics and Microelectronics, Zhengzhou University, Zhengzhou 450052, Henan, P.R. China*

[c] *Zhejiang Laboratory, Hangzhou, Zhejiang, P.R. China.*
E-mail: yang_shuxiang@zhejianglab.com

† Electronic supplementary information (ESI) available. See DOI: https://doi.org/10.1039/d4cp00191e

‡ These authors contributed equally to this work.

This journal is © the Owner Societies 2024

Phys. Chem. Chem. Phys., 2024, **26**, 16963–16971 | **16963**

experiment[44]), or even quaternary borides $RbYbB_6C_6$ and $RbBaB_6C_6$ (both with $T_c \approx 71$ K at ambient pressure, theory[45]).

There have been extensive efforts in searching for similar metal-boride superconductors since the discovery of MgB_2 as presented above. Unfortunately, the outcomes have been discouraging in that the T_c values of most metal borides are much lower than that of MgB_2. However, the recent experimental discovery of superconducting MoB_2 with $T_c = 32$ K at 100 GPa [26] has ignited further enthusiasm in looking for superconducting transition-metal borides at lower pressures or even at ambient pressure. In addition, the superconducting mechanism of MoB_2 is suggested to be very different from MgB_2. In MgB_2 the B-p electrons play a dominant role in its superconductivity,[46,47] while in MoB_2 its Mo-4d electrons contribute majorly.[26,48] This raises two essential questions: (1) Can we find other superconducting transition-metal borides neighboring to MoB_2, with T_c at least above 10 K and at moderate pressures? (2) Does the superconducting mechanism of MoB_2 apply to other superconducting transition-metal borides? To answer these two questions, we decided to work on borides of technetium, which comes immediately after molybdenum in the periodic table.

Although technetium is rare in nature, technetium-based compounds have been investigated in multiple disciplines in the past. $ATcO_3$ perovskites (where A = Ca, Sr, Ba) have attracted extensive interest due to their extremely high antiferromagnetic Néel temperatures (750–1200 K).[49–52] First-principle calculations have predicted a stable structure of ternary compound Tc_2AlB_2 with $Cmcm$ symmetry at ambient pressure.[53] Recently, technetium hydrides were theoretically predicted and then experimentally synthesized under high pressure.[54,55]

Technetium borides have been extensively investigated due to their outstanding mechanical properties.[56–76] Three technetium borides have long been synthesized experimentally at ambient pressure,[56] Tc_3B ($Cmcm$) with an orthorhombic structure, and Tc_7B_3 ($P6_3/mmc$) and TcB_2 ($P6_3/mmc$, Vickers hardness 38.4 GPa [76] or 39.4 GPa [75]) with hexagonal structures. Later theoretical calculations also proposed three stoichiometries of TcB, TcB_3 and TcB_4.[62,70–75] First-principle DFT calculations by Li et $al.$[62] suggested that hexagonal TcB ($P\bar{6}m2$) could be energetically stable. Structural searches by Wu et $al.$[71] found a thermodynamically stable TcB ($Cmcm$) structure above 8 GPa. Later structural searches by Zhang et $al.$[72] led to the argument that TcB ($P\bar{3}m1$, Vickers hardness 30.3 GPa) could be energetically more stable than the above two structures. Structural predictions by Van Der Geest et $al.$[70] suggest there are two thermodynamically stable structures, TcB ($Pnma$) and TcB_4 ($P6_3/mmc$), at 30 GPa. First-principle DFT calculations by Miao et $al.$[74] reported a thermodynamically stable TcB_3 structure ($P\bar{6}m2$, Vickers hardness 29 GPa) above 4 GPa. Structural searches by Ying et $al.$[73,75] suggested two structures, TcB_3 ($P\bar{6}m2$, Vickers hardness 30.7 GPa) and TcB_4 ($P6_3/mmc$, Vickers hardness 32.4 GPa), that are thermodynamically stable at 0 and 100 GPa, respectively. However, the discussions of possible superconductivity in technetium borides are totally absent.

In this paper, we choose to search the technetium–boron binary system for new superconductors. A comprehensive phase diagram of all thermodynamically stable technetium borides up to 180 GPa has been derived. We also found five superconducting technetium borides possessing metastable states for the first time, including TcB ($P6_3/mmc$), TcB_2 ($P6/mmm$), Tc_2B ($I4/mcm$), Tc_3B ($P4/mmm$) and TcB ($Cmcm$), that remain dynamically stable at low or even ambient pressures. The mechanical properties of these superconducting technetium borides have been investigated as well.

2 Methods

The structure prediction for technetium–boron binary crystals is performed by the CALYPSO package.[77] The crystal structures and the X-ray diffraction (XRD) patterns are generated by the VESTA package. The electronic structures and the phonon properties are calculated using the QUANTUM-ESPRESSO (QE) package.[78] The plane-wave kinetic-energy cutoff and the charge density energy cutoff are 100 Ry and 400 Ry, respectively. An optimized norm-conversing pseudopotential with valence electron configurations of Tc-$4p^6$ $4d^5$ $5s^2$ and B-$2s^2$ $2p^1$ and a Methfessel–Paxton smearing[79] width of 0.02 Ry is used.

The dynamic matrix and the electron–phonon coupling (EPC) constant λ are calculated using the density functional perturbation theory.[80] The superconducting transition temperature is estimated following the Allen-Dynes modified McMillan equation,[81]

$$T_c = \frac{\omega_{\log}}{1.2} \exp\left[-\frac{1.04(1+\lambda)}{\lambda - \mu^*(1+0.62\lambda)}\right], \qquad (1)$$

in which λ is the average EPC parameter, $\omega_{\log}$ is the logarithmic average frequency, and the Coulomb pseudopotential[82] $\mu^* = 0.12$. Mechanical properties including Vickers hardness are estimated following models by Chen et $al.$ and Tian et $al.$[83,84] Calculation details are given in the ESI.†

3 Results and discussion

3.1 Convex hull and phase diagram

We have done variable-composition and fixed-composition structure searches in the Tc–B system at pressures of 0, 90 and 180 GPa. Thermodynamically stable structures and the derived composition–pressure phase diagram are presented in Fig. 1. Three existing technetium borides at ambient pressure, Tc_3B ($Cmcm$), Tc_7B_3 ($P6_3/mmc$) and TcB_2 ($P6_3/mmc$), have been successfully identified. Tc_3B ($Cmcm$) is thermodynamically stable up to 180 GPa in our study. In contrast, Tc_7B_3 ($P6_3/mmc$) and TcB_2 ($P6_3/mmc$) stop being energetically favorable above 60 GPa and 139 GPa, respectively, and a new TcB_2 ($I4_1/amd$) thermodynamically stable phase shows up above 170 GPa. Two previously predicted structures, TcB_3 ($P\bar{6}m2$)[73,74] and TcB_4 ($P6_3/mmc$),[70,75] also have been found in our calculations, and these structures are thermodynamically stable above 2 and 35 GPa, respectively. We found a TcB ($P2_1$) structure that is thermodynamically stable above 24 GPa, then transfers into a $Pmn2_1$ structure at 63 GPa, and finally into the previously predicted $Pnma$ structure[70] at
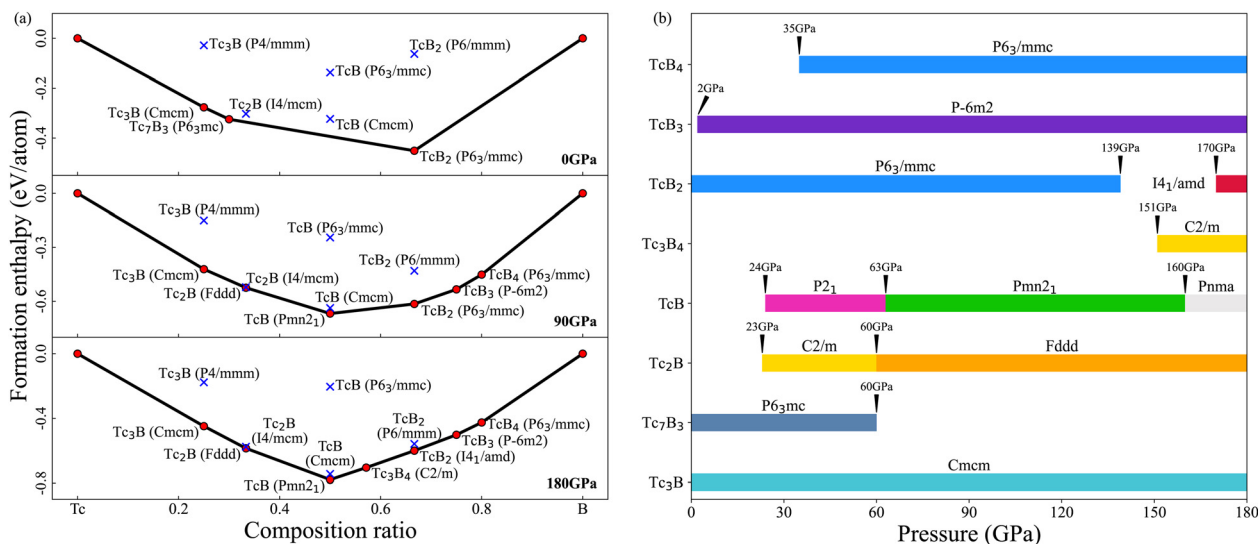
Fig. 1 (a) Formation enthalpies of predicted structures in the technetium–boron binary system at 0 GPa, 90 GPa and 180 GPa. Thermodynamically stable structures are marked by red-filled dots on the convex hull (black solid line); thermodynamically metastable structures are marked by a blue 'x'. The composition ratio is defined by $N_B/(N_{T_c} + N_B)$, where N_B and N_{T_c} represent the number of atoms in the formula unit. (b) Composition–pressure phase diagram of thermodynamically stable structures in the technetium–boron binary system.

160 GPa. We also discovered technetium borides with two new stoichiometries, Tc_3B_4 and Tc_2B. Tc_3B_4 ($C2/m$) is thermodynamically stable above 151 GPa. The Tc_2B ($C2/m$) structure is thermodynamically stable above 23 GPa, then transfers into an $Fddd$ structure at 60 GPa. The crystal structure information and the XRD patterns of all thermodynamically stable phases are presented in Table S4 and Fig. S4 of the ESI.†

3.2 Superconductivity of thermodynamically metastable technetium borides

We have examined potential superconductivity in the predicted technetium borides, including all thermodynamically stable structures and the thermodynamically metastable structures within a range of 300 meV above the convex hull. A total of five thermodynamically metastable technetium borides have been found to be superconducting at 180 GPa, including TcB_2 ($P6/mmm$, 42 meV per atom above the hull), TcB ($P6_3/mmc$, 255 meV per atom above the hull), Tc_2B ($I4/mcm$, 2 meV per

atom above the hull), Tc_3B ($P4/mmm$, 248 meV per atom above the hull) and TcB ($Cmcm$, 25 meV per atom above the hull). These five superconducting technetium borides stay dynamically stable at decreased pressures. The minimum dynamically stable pressures of TcB_2 ($P6/mmm$) and TcB ($Cmcm$) are 20 and 30 GPa, respectively, while TcB ($P6_3/mmc$), Tc_2B ($I4/mcm$) and Tc_3B ($P4/mmm$) are dynamically stable even at ambient pressure.

The superconducting transition temperatures of the technetium borides are presented in Fig. 2, together with the transition temperatures of other known superconducting metal borides that have been measured experimentally for benchmarking. As shown in Fig. 2b, the superconducting transition temperatures of the technetium borides in our study increase at decreased pressure. Although the superconducting transition temperatures of all five technetium borides are always lower than these of MgB_2[15] and MoB_2,[26] they are higher than the superconducting transition temperatures of other metal borides in Fig. 2a at their lowest dynamically stable pressures. In addition, TcB_2 ($P6/mmm$) and TcB
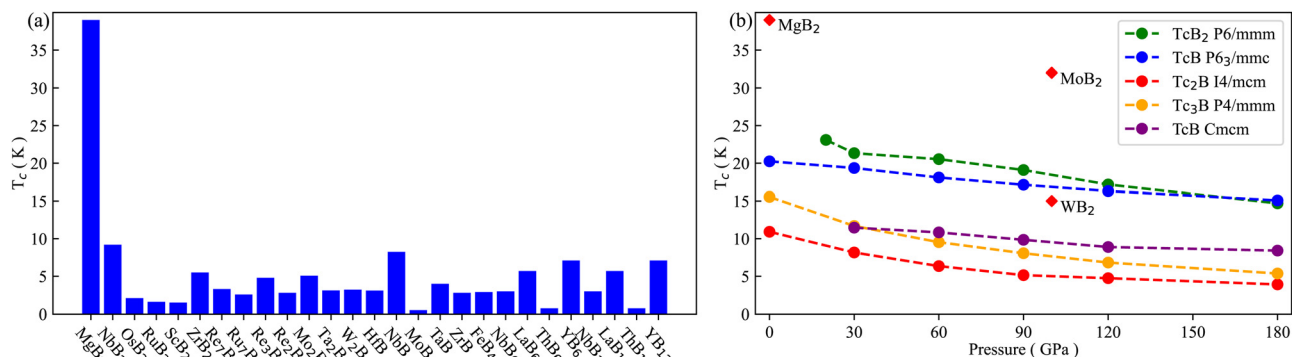

Fig. 2 (a) Superconducting transition temperatures of metal borides at ambient pressure measured experimentally. (b) Superconducting transition temperatures of TcB_2 ($P6/mmm$), TcB ($P6_3/mmc$), Tc_2B ($I4/mcm$), Tc_3B ($P4/mmm$) and TcB ($Cmcm$) as a function of pressure, together with the superconducting transition temperatures of MgB_2 at ambient pressure, and MoB_2 and WB_2 at 100 GPa, measured experimentally (red diamonds).

This journal is © the Owner Societies 2024

Phys. Chem. Chem. Phys., 2024, **26**, 16963–16971 | **16965**

Table 1 Total electronic density of states (DOS) at the Fermi level $N(E_F)$, EPC parameter λ, logarithmic average frequency $\omega_{\log}$, and superconducting transition temperature T_c of the superconducting technetium borides at their lowest dynamically stable pressures

Formula	Space group	P (GPa)	$N(E_F)$ (states per eV per f.u.)	λ	$\omega_{\log}$ (cm^{-1})	T_c (K)
TcB$_2$	$P6/mmm$	20	1.41	1.85	125.1	23.1
TcB	$P6_3/mmc$	0	1.63	1.56	126.1	20.2
Tc$_2$B	$I4/mcm$	0	1.75	0.85	165.1	10.9
Tc$_3$B	$P4/mmm$	0	2.85	0.92	162.9	12.9
TcB	$Cmcm$	30	1.05	0.96	135.5	11.5

($P6_3/mmc$) have higher superconducting transition temperatures at 100 GPa than WB$_2$ with $T_c = 15$ K.[23]

We also present the superconducting transition temperatures of the five technetium borides at their lowest dynamically stable pressures, together with their total electronic DOS at the Fermi level $N(E_F)$, the EPC parameter λ and the logarithmic average frequency $\omega_{\log}$ in Table 1. TcB$_2$ ($P6/mmm$) has the highest superconducting transition temperature of 23.1 K at 20 GPa, which comes from its largest EPC parameter of $\lambda = 1.85$. In contrast, TcB ($Cmcm$) has a much lower superconducting transition temperature of 11.5 K at 30 GPa due to its small EPC parameter of $\lambda = 0.96$. The superconducting transition temperatures of TcB ($P6_3/mmc$), Tc$_2$B ($I4/mcm$) and Tc$_3$B ($P4/mmm$) at 0 GPa are 20.2, 10.9, and 12.9 K, respectively. Although the EPC parameters λ of these metastable technetium borides are not small, their logarithmic average frequencies $\omega_{\log}$ are rather low with a maximum of 165.1 cm^{-1}, which limits their superconducting transition temperature. This is in sharp contrast with MgB$_2$, which has a smaller λ value of 0.87 but a much larger $\omega_{\log}$ value of 504 cm^{-1}, and the highest BCS-type superconducting transition temperature of 39 K at ambient pressure.[85]

The thermodynamically metastable nature of the discovered superconducting technetium borides doesn't necessarily exclude their experimental synthesis. Metastable materials have long been synthesized and implemented,[86] typically like fullerene C$_{60}$. As for superconductors, DFT calculations predict NdH$_9$ ($P6_3/mmc$) has a formation enthalpy that is 35 meV per atom above the convex hull at 150 GPa, yet it has been successfully synthesized with $T_c \approx 4.5$ K.[87] Several metastable borides have been predicted to be superconducting in recent structural searches. Xia *et al.* discovered thermodynamically metastable CB$_6$ with a superconducting transition temperature of 12.5 K at ambient pressure.[33] Zhang *et al.* also found thermodynamically metastable RbB$_6$ ($Pm\bar{3}m$) and RbB$_8$ ($Immm$) with superconducting transition temperatures of 7.3–11.6 and 4.8–7.5 K at ambient pressure, respectively.[37] These works further validate the importance and necessity of our discoveries of superconducting technetium borides.

3.3 Crystal structures

The crystal structures of the five superconducting technetium borides in our study are presented in Fig. 3. TcB$_2$ ($P6/mmm$) shares exactly the same crystal structure with MgB$_2$ and MoB$_2$. TcB ($P6_3/mmc$) has a TiAs-type structure, in which the rhombus

Tc-layers are AB-stacking along the c-axis and the rhombus B-layers are sandwiched between the neighbouring Tc-layers. Tc$_3$B ($P4/mmm$) has square Tc-layers stacking in an ABB-pattern along the c-axis, and the square B-layers are located between the two Tc-layers of the BB-pattern. Tc$_2$B ($I4/mcm$) consists of square Tc-layers AB-stacking along the c-axis, where the neighbouring Tc-layers are twisted by 37.2 degrees. The B-layers in Tc$_2$B ($I4/mcm$) are sandwiched between the neighbouring Tc-layers as well. In TcB ($Cmcm$), the square Tc-layers stack in an ABCD-pattern along the b-axis, and the B atoms form zig-zag chains along the c-axis between the AB and CD Tc-layers. The angle of the zig-zag chain of the B atoms is around 108.8 degrees. Crystal structure information and the XRD patterns of the superconducting technetium borides are presented in Table S3 and Fig. S3 of the ESI.†

3.4 Electronic structures

The electronic DOS of superconducting technetium borides at their lowest stabilizing pressure are presented in the left column of Fig. 4. The electronic DOS of all technetium borides share certain features. The total DOS at the Fermi level are dominated by the states of the Tc-4d bands. Although the B-2p DOS have considerable weight away the Fermi level, its contribution is minor at the Fermi level, if not zero. The B-2s DOS almost vanish around the Fermi level, which makes the B-2s bands almost irrelevant for electronic conduction. Our DOS results for technetium borides have a close resemblance to those for the transition-metal boride MoB$_2$,[26] while they are in obvious contrast to results for the alkali-earth-metal boride MgB$_2$ [46,47] and the alkali-metal boride RbB$_6$.[37] In both MgB$_2$ [46,47] and RbB$_6$,[37] the major DOS at the Fermi level are contributed by the B-p bands. But in both the superconducting technetium borides of our study and MoB$_2$,[26] the 4d electronic states play dominant roles around the Fermi level.

The electronic band structures, the partial DOS of the Tc-4d orbitals and the Fermi surfaces of the superconducting technetium borides are presented in Fig. S2 of the ESI.† For all five superconducting technetium borides, either their band structure or their Fermi surface show obvious electronic dispersion in three dimensions. Typically, for example, TcB$_2$, which shares the same crystal structure as MgB$_2$ and MoB$_2$, has a three-dimensional Fermi surface like MoB$_2$,[26,88] while being distinct from the quasi-two-dimensional Fermi surface of MgB$_2$.[47,89]

3.5 Dynamic stability and electron–phonon coupling

The phonon spectra, the PHDOS, the Eliashberg functional $\alpha^2F(\omega)$ and the corresponding integrated EPC constant λ of the superconducting technetium borides at their lowest dynamically stable pressures are presented in the right column of Fig. 4. There is no sign of an imaginary frequency in the phonon spectra of all five superconducting technetium borides, which proves the dynamic stability of these structures at the corresponding pressures. The distribution of the PHDOS and the Eliashberg spectral functional $\alpha^2F(\omega)$ of the superconducting technetium borides show clear separation between the low-frequency phonon modes of the heavier Tc atoms and the high frequency phonon modes of the lighter B atoms. This enables us to separate the integrated
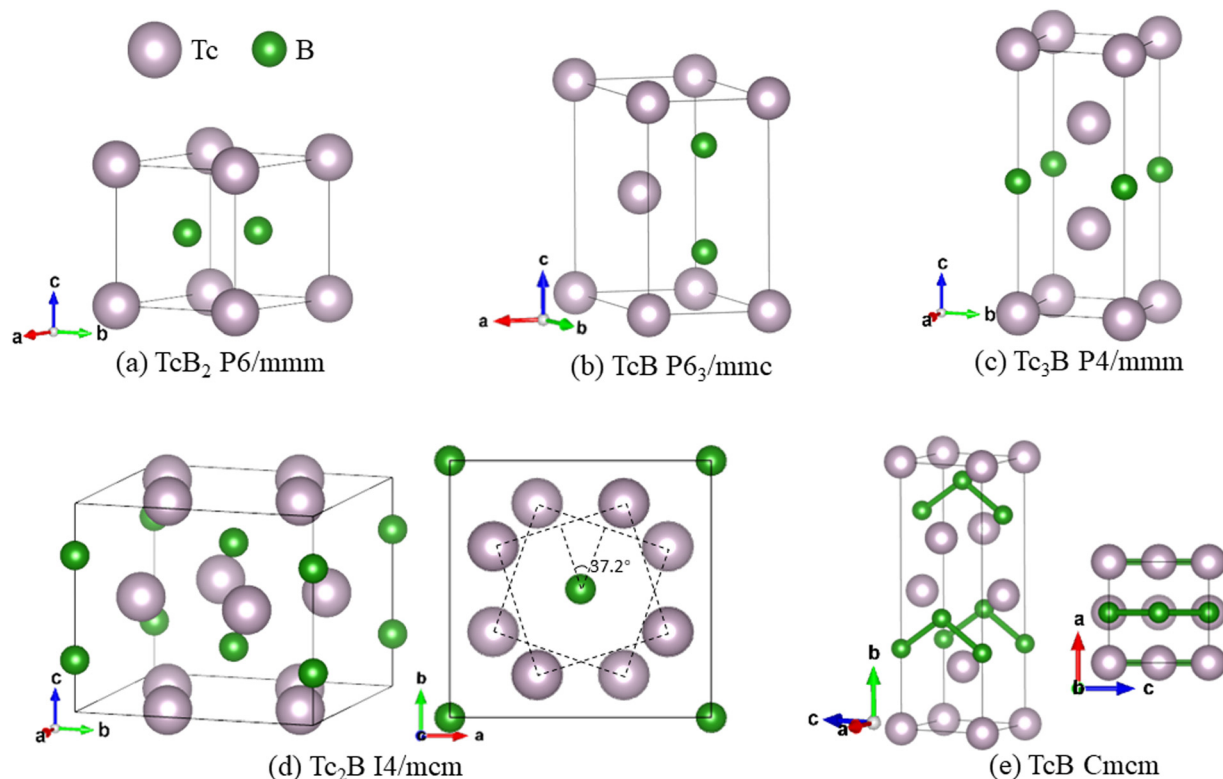
16966 | *Phys. Chem. Chem. Phys.*, 2024, **26**, 16963–16971

This journal is © the Owner Societies 2024

Fig. 3 Crystal structures of superconducting technetium borides. (a) TcB$_2$ (P6/mmm), (b) TcB (P6$_3$/mmc), (c) Tc$_2$B (I4/mcm), (d) Tc$_3$B (P4/mmm) and (e) TcB (Cmcm). The technetium and boron atoms are represented by spheres of coral and green colors, respectively.

EPC constant λ into two parts, the EPC from the Tc atoms λ_{T_c}, and the EPC from the B atoms λ_B. The ratio of EPC from oscillation of the Tc atoms relative to the total EPC, λ_{T_c}/λ, are 0.883, 0.910, 0.873, 0.907 and 0.911 for TcB$_2$ (P6/mmm), TcB (P6$_3$/mmc), Tc$_2$B (I4/mcm), Tc$_3$B (P4/mmm) and TcB (Cmcm), respectively. It indicates that superconductivity in these five technetium borides mainly originates from the coupling between the Tc-4d electrons and the low frequency phonon modes of the Tc atoms.

The superconducting mechanism of our predicted technetium borides is similar to that in the transition-metal boride MoB$_2$, whose superconductivity mainly originates from the coupling between the Mo-4d electrons and the low frequency Mo-phonon modes.[26] However, the superconducting scenarios in the alkali-earth-metal boride MgB$_2$[46,47] and the alkali-metal boride RbB$_6$[37] are very different in that the couplings between the B-2p electrons and the high-frequency B-phonon modes play dominant roles. At least three isotopes of technetium have reasonably long half-lives (Tc-97, Tc-98 and Tc-99 at 4.2×10^6, 6.6×10^6 and 2.13×10^5 years, respectively). Therefore, we suggest experiments on the isotope effects of technetium to examine our prediction.

Observations in the phonon spectra, PHDOS and EPC of the superconducting technetium borides are consistent with their relatively smaller logarithmic average frequency $\omega_{\log}$ as listed in Table 1, since Tc atoms are much heavier than B atoms. The enhanced λ plus small $\omega_{\log}$ characteristics of TcB$_2$ have also been seen in the iso-structural superconductor TlBi$_2$ of heavy atomic mass,[90] with $\lambda = 1.4$, $\omega_{\log} = 37$ cm^{-1} and rather low

$T_c = 5.5$ K. Recent work suggests that the introduction of hydrogen atoms into the non-superconducting transition-metal boride Ti$_2$B$_2$ will result in superconducting Ti$_2$B$_2$H$_4$ ($T_c = 48.6$ K at ambient pressure), through expansion of the frequency range of the phonon spectrum and consequently enlarged electron–phonon coupling.[91] Similar hydrogenation probably helps in elevating the superconducting transition temperatures of technetium borides by the enlarged $\omega_{\log}$.

Another interesting observation on the discovered super-conducting technetium borides is that the Fermi levels of TcB$_2$ and TcB fall closely above the peak positions of their DOS, as shown in Fig. 4. Since the EPC in technetium borides is controlled by the coupling between the Tc-4d electrons and the oscillation of the Tc atoms, slight hole-doping could lower the Fermi level, thus enhancing the effective number of electrons participating in the superconducting pairing and therefore increasing the superconducting transition temperatures.

3.6 Hardness

We also calculated the Vickers hardness of the discovered superconducting technetium borides as presented in Table 2. At ambient pressure, TcB (P6$_3$/mmc), Tc$_2$B (I4/mcm) and Tc$_3$B (P4/mmm) have Vickers hardness values of 2.8–4.8, 11.8–13.0 and 10.0–11.3 GPa, respectively. The Vickers hardness values of TcB$_2$ (P6/mmm) and TcB (Cmcm) are 9.8–11.3 GPa and 12.2–13.7 GPa at pressures of 20 and 30 GPa, respectively. The superconducting technetium borides in our study have lower hardness values than
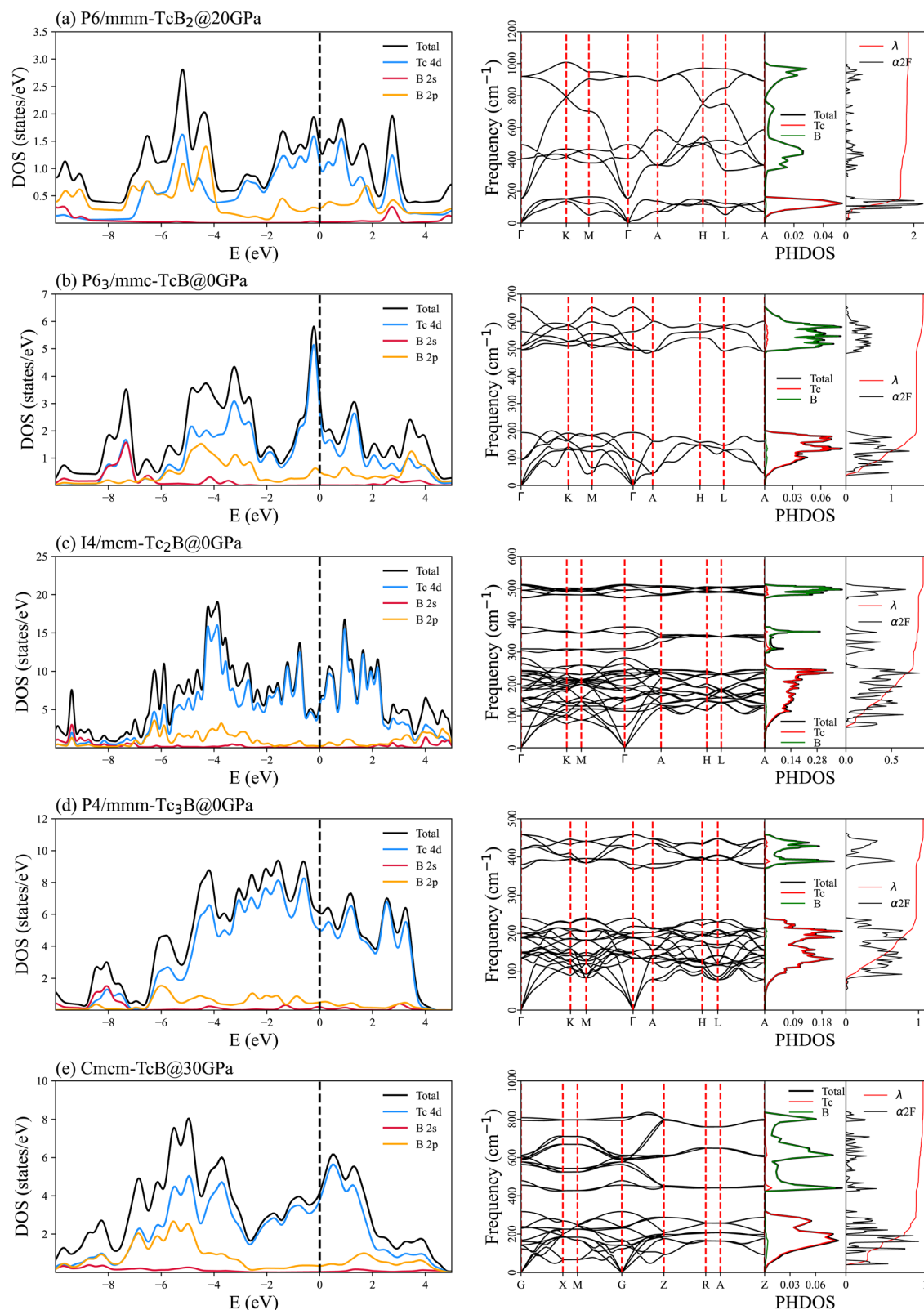
This journal is © the Owner Societies 2024

Phys. Chem. Chem. Phys., 2024, **26**, 16963–16971 | **16967**

Fig. 4 Total and partial electronic DOS, phonon dispersion relation, phonon density of states (PHDOS), Eliashberg functional $\alpha^2F(\omega)$ and integrated EPC parameter $\lambda(\omega)$ of superconducting technetium borides at their lowest dynamically stable pressures. From top to bottom: (a) TcB$_2$ ($P6/mmm$, 20 GPa), (b) TcB ($P6_3/mmc$, 0 GPa), (c) Tc$_2$B ($I4/mcm$, 0 GPa), (d) Tc$_3$B ($P4/mmm$, 0 GPa) and (e) TcB ($Cmcm$, 30 GPa).

16968 | *Phys. Chem. Chem. Phys.*, 2024, **26**, 16963–16971

This journal is © the Owner Societies 2024

Table 2 Vickers hardness of superconducting technetium borides at their lowest dynamically stable pressures

Formula	Space Group	P (GPa)	$H_{v,\text{Chen}}$[83] (GPa)	$H_{v,\text{Tian}}$[84] (GPa)
TcB_2	$P6/mmm$	20	10.6	12.0
TcB	$P6_3/mmc$	0	2.8	4.8
Tc_2B	$I4/mcm$	0	11.8	13.0
Tc_3B	$P4/mmm$	0	10.0	11.3
TcB	$Cmcm$	30	12.2	13.7

those previously stated for superconducting superhard borides, for example RbB_6 ($Pm\bar{3}m$, Vickers hardness of 19.7 GPa at ambient pressure) and RbB_8 ($Immm$, Vickers hardness of 36.9 GPa at ambient pressure).[37] Other mechanical parameters including elastic constants C_{ij}, bulk modulus B, and shear modulus G at their lowest dynamically stable pressures were also calculated. Mechanical stability criteria[92] related to the elastic constants of these superconducting technetium borides are fulfilled as presented in the ESI.†

4 Conclusions

In summary, we have conducted thorough structural searches in the technetium–boron binary system. An updated composition–pressure phase diagram for technetium borides at up to 180 GPa have been derived, including two new stoichiometries as Tc_3B_4 and Tc_2B. More importantly, we also found five unprecedented superconducting technetium borides that remain dynamically stable at moderate or even ambient pressures. Among these thermodynamically metastable superconducting technetium borides, TcB_2 ($P6/mmm$) has the highest superconducting transition temperature of 23.1 K at 20 GPa, and TcB ($P6_3/mmc$) has the highest superconducting transition temperature of 20.2 K at ambient pressure. The superconductivity in these technetium borides mainly originates from the coupling between the dominant presence of Tc-4d electronic states around the Fermi level and the low-frequency vibrational modes of the technetium atoms, which are closely analogous to another transition-metal-boride MoB_2. Our calculations not only identified that superconducting TcB_2 ($P6/mmm$) has the same crystal structure as MgB_2 and MoB_2, but also led to the discovery of a series of superconducting technetium borides with diversified crystal structures. This work proves the rich structures and stoichiometries in superconducting technetium borides at high pressures, thus indicating the necessity for extended research in the discovery of new superconducting transition-metal borides.

Conflicts of interest

There are no conflicts of interest to declare.

Acknowledgements

References

1 H. K. Onnes, *Proceedings Koninklijke Akademie van Wetenschappen te Amsterdam*, 1911, pp. 1274–1276.
2 C. J. Pickard and R. Needs, *J. Phys.: Condens. Matter*, 2011, **23**, 053201.
3 Y. Wang, J. Lv, L. Zhu and Y. Ma, *Comput. Phys. Commun.*, 2012, **183**, 2063–2070.
4 A. R. Oganov and C. W. Glass, *J. Chem. Phys.*, 2006, **124**, 244704.
5 F. Giustino, *Rev. Mod. Phys.*, 2017, **89**, 015003.
6 D. Duan, Y. Liu, F. Tian, D. Li, X. Huang, Z. Zhao, H. Yu, B. Liu, W. Tian and T. Cui, *Sci. Rep.*, 2014, **4**, 6968.
7 A. Drozdov, M. Eremets, I. Troyan, V. Ksenofontov and S. I. Shylin, *Nature*, 2015, **525**, 73–76.
8 H. Liu, I. I. Naumov, R. Hoffmann, N. Ashcroft and R. J. Hemley, *Proc. Natl. Acad. Sci. U. S. A.*, 2017, **114**, 6990–6995.
9 Z. M. Geballe, H. Liu, A. K. Mishra, M. Ahart, M. Somayazulu, Y. Meng, M. Baldini and R. J. Hemley, *Angew. Chem., Int. Ed.*, 2018, **57**, 688–692.
10 M. Somayazulu, M. Ahart, A. K. Mishra, Z. M. Geballe, M. Baldini, Y. Meng, V. V. Struzhkin and R. J. Hemley, *Phys. Rev. Lett.*, 2019, **122**, 027001.
11 A. Drozdov, P. Kong, V. Minkov, S. Besedin, M. Kuzovnikov, S. Mozaffari, L. Balicas, F. Balakirev, D. Graf and V. Prakapenka, *Nature*, 2019, **569**, 528–531.
12 X. Tao, A. Yang, S. Yang, Y. Quan and P. Zhang, *Sci. Bull.*, 2023, **68**, 1372–1378.
13 A. Yang, X. Tao, Y. Quan and P. Zhang, *Phys. B*, 2024, **677**, 415706.
14 W. Sun, B. Chen, X. Li, F. Peng, A. Hermann and C. Lu, *Phys. Rev. B*, 2023, **107**, 214511.
15 J. Nagamatsu, N. Nakagawa, T. Muranaka, Y. Zenitani and J. Akimitsu, *Nature*, 2001, **410**, 63–64.
16 H. J. Choi, S. G. Louie and M. L. Cohen, *Phys. Rev. B: Condens. Matter Mater. Phys.*, 2009, **80**, 064503.
17 Z. Yu, T. Bo, B. Liu, Z. Fu, H. Wang, S. Xu, T. Xia, S. Li, S. Meng and M. Liu, *Phys. Rev. B*, 2022, **105**, 214517.
18 J. Schirber, D. Overmyer, B. Morosin, E. Venturini, R. Baughman, D. Emin, H. Klesnar and T. Aselage, *Phys. Rev. B: Condens. Matter Mater. Phys.*, 1992, **45**, 10787.
19 A. Yamamoto, C. Takao, T. Masui, M. Izumi and S. Tajima, *Phys. C*, 2002, **383**, 197–206.

This journal is © the Owner Societies 2024

Phys. Chem. Chem. Phys., 2024, **26**, 16963–16971 | **16969**

20 H. Takeya, K. Togano, Y. S. Sung, T. Mochiku and K. Hirata, *Phys. C*, 2004, **408–410**, 144–145.

21 Y. Singh, A. Niazi, M. D. Vannette, R. Prozorov and D. C. Johnston, *Phys. Rev. B: Condens. Matter Mater. Phys.*, 2007, **76**, 214510.

22 G. V. Samsonov, *Handbook of Refractory Compounds*, Springer, New York, 1980.

23 C. Pei, J. Zhang, C. Gong, Q. Wang, L. Gao, Y. Zhao, S. Tian, W. Cao, C. Li, Z.-Y. Lu, H. Lei, K. Liu and Y. Qi, *Sci. China: Phys., Mech. Astron.*, 2022, **65**, 287412.

24 L. Leyarovska and E. Leyarovski, *J. Less-Common Met.*, 1979, **67**, 249–255.

25 X. Liang, A. Bergara, Y. Xie, L. Wang, R. Sun, Y. Gao, X.-F. Zhou, B. Xu, J. He, D. Yu, G. Gao and Y. Tian, *Phys. Rev. B*, 2020, **101**, 014112.

26 C. Pei, J. Zhang, Q. Wang, Y. Zhao, L. Gao, C. Gong, S. Tian, R. Luo, M. Li, W. Yang, Z.-Y. Lu, H. Lei, K. Liu and Y. Qi, *Natl. Sci. Rev.*, 2023, **10**, nwad034.

27 C. Buzea and T. Yamashita, *Supercond. Sci. Technol.*, 2001, **14**, R115.

28 A. Kawano, Y. Mizuta, H. Takagiwa, T. Muranaka and J. Akimitsu, *J. Phys. Soc. Jpn.*, 2003, **72**, 1724–1728.

29 A. N. Kolmogorov, S. Shah, E. R. Margine, A. F. Bialon, T. Hammerschmidt and R. Drautz, *Phys. Rev. Lett.*, 2010, **105**, 217003.

30 H. Gou, N. Dubrovinskaia, E. Bykova, A. A. Tsirlin, D. Kasinathan, W. Schnelle, A. Richter, M. Merlini, M. Hanfland, A. M. Abakumov, D. Batuk, G. Van Tendeloo, Y. Nakajima, A. N. Kolmogorov and L. Dubrovinsky, *Phys. Rev. Lett.*, 2013, **111**, 157002.

31 H. Xie, H. Wang, F. Qin, W. Han, S. Wang, Y. Wang, F. Tian and D. Duan, *Matter Radiat. Extremes*, 2023, **8**, 058404.

32 L. Wu, B. Wan, H. Liu, H. Gou, Y. Yao, Z. Li, J. Zhang, F. Gao and H.-K. Mao, *J. Phys. Chem. Lett.*, 2016, **7**, 4898–4904.

33 K. Xia, M. Ma, C. Liu, H. Gao, Q. Chen, J. He, J. Sun, H.-T. Wang, Y. Tian and D. Xing, *Mater. Today Phys.*, 2017, **3**, 76–84.

34 L. Duan, J. Su, N. Gong, B. Wan, P. Chen, P. Zhou, Z. Wang, Z. Li and L. Wu, *Dalton Trans.*, 2019, **48**, 14299–14305.

35 J. Du, X. Li and F. Peng, *Phys. Chem. Chem. Phys.*, 2022, **24**, 10079–10084.

36 S. Han, L. Yu, Y. Liu, B. Zhao, C. Wang, X. Chen, Y. Zhang, R. Yu and X. Liu, *Adv. Funct. Mater.*, 2023, **33**, 2213377.

37 P. Zhang, Y. Tian, Y. Yang, H. Liu and G. Liu, *Phys. Rev. Res.*, 2023, **5**, 013130.

38 R. Lortz, Y. Wang, U. Tutsch, S. Abe, C. Meingast, P. Popovich, W. Knafo, N. Shitsevalova, Y. B. Paderno and A. Junod, *Phys. Rev. B: Condens. Matter Mater. Phys.*, 2006, **73**, 024512.

39 L. Ma, X. Yang, G. Liu, H. Liu, G. Yang, H. Wang, J. Cai, M. Zhou and H. Wang, *Phys. Rev. B*, 2021, **104**, 174112.

40 Y. Liang, M. Xu, S. Lin, X. Yuan, Z. Qu, J. Hao and Y. Li, *J. Mater. Chem. C*, 2021, **9**, 13782–13788.

41 G. Akopov, W. H. Mak, D. Koumoulis, H. Yin, B. Owens-Baird, M. T. Yeung, M. H. Muni, S. Lee, I. Roh, Z. C. Sobell, P. L. Diaconescu, R. Mohammadi, K. Kovnir and R. B. Kaner, *J. Am. Chem. Soc.*, 2019, **141**, 9047–9062.

42 J. Teyssier, A. B. Kuzmenko, D. van der Marel, F. Marsiglio, A. B. Liashchenko, N. Shitsevalova and V. Filippov, *Phys. Rev. B: Condens. Matter Mater. Phys.*, 2007, **75**, 134503.

43 B. T. Matthias, T. H. Geballe, K. Andres, E. Corenzwit, G. W. Hull and J. P. Maita, *Science*, 1968, **159**, 530.

44 L. Zhu, H. Liu, M. Somayazulu, Y. Meng, P. A. Guńka, T. B. Shiell, C. Kenney-Benson, S. Chariton, V. B. Prakapenka, H. Yoon, J. A. Horn, J. Paglione, R. Hoffmann, R. E. Cohen and T. A. Strobel, *Phys. Rev. Res.*, 2023, **5**, 013012.

45 Q. Duan, L. Zhan, J. Shen, X. Zhong and C. Lu, *Phys. Rev. B*, 2024, **109**, 054505.

46 J. M. An and W. E. Pickett, *Phys. Rev. Lett.*, 2001, **86**, 4366–4369.

47 J. Kortus, I. I. Mazin, K. D. Belashchenko, V. P. Antropov and L. L. Boyer, *Phys. Rev. Lett.*, 2001, **86**, 4656–4659.

48 C. Zhou, H. Yu, Z. Zhang, Z. Yu, J. Zhu, K. Bao and T. Cui, *Phys. Rev. B*, 2024, **109**, 064502.

49 M. Avdeev, G. J. Thorogood, M. L. Carter, B. J. Kennedy, J. Ting, D. J. Singh and K. S. Wallwork, *J. Am. Chem. Soc.*, 2011, **133**, 1654–1657.

50 C. Franchini, T. Archer, J. He, X.-Q. Chen, A. Filippetti and S. Sanvito, *Phys. Rev. B: Condens. Matter Mater. Phys.*, 2011, **83**, 220402.

51 E. E. Rodriguez, F. Poineau, A. Llobet, B. J. Kennedy, M. Avdeev, G. J. Thorogood, M. L. Carter, R. Seshadri, D. J. Singh and A. K. Cheetham, *Phys. Rev. Lett.*, 2011, **106**, 067201.

52 J. Mravlje, M. Aichhorn and A. Georges, *Phys. Rev. Lett.*, 2012, **108**, 197202.

53 H. Zhang, J. Wang, M. Khazaei, F. Guegan and G. Frapper, *Phys. Chem. Chem. Phys.*, 2021, **23**, 22086–22095.

54 X. Li, H. Liu and F. Peng, *Phys. Chem. Chem. Phys.*, 2016, **18**, 28791–28796.

55 D. Zhou, D. V. Semenok, M. A. Volkov, I. A. Troyan, A. Y. Seregin, I. V. Chepkasov, D. A. Sannikov, P. G. Lagoudakis, A. R. Oganov and K. E. German, *Phys. Rev. B*, 2023, **107**, 064102.

56 W. Trzebiatowski and J. Rudzinski, *J. Less-Common Met.*, 1964, **6**, 244–245.

57 D. Armstrong, *J. Less-Common Met.*, 1979, **67**, 191–203.

58 A. Pallas and K. Larsson, *J. Phys. Chem. B*, 2006, **110**, 5367–5371.

59 Y. Wang, *Appl. Phys. Lett.*, 2007, **91**, 101904.

60 M. Wang, Y. Li, T. Cui, Y. Ma and G. Zou, *Appl. Phys. Lett.*, 2008, **93**, 101905.

61 S. Aydin and M. Simsek, *Phys. Rev. B: Condens. Matter Mater. Phys.*, 2009, **80**, 134107.

62 J. Li, X. Wang, K. Liu, Y. Sun, L. Chen and H. Yang, *Phys. B*, 2010, **405**, 4659–4663.

63 W. Chen and J. Jiang, *Solid State Commun.*, 2010, **150**, 2093–2096.

64 W. Jie Zhao and B. Xu, *Comput. Mater. Sci.*, 2012, **65**, 372–376.

65 E. Deligoz, K. Çolakoğlu, H. B. Ozisik and Y. O. Ciftci, *Solid State Sci.*, 2012, **14**, 794–800.

66 M. Zhong, X. Yu Kuang, Z.-H. Wang, P. Shao, L.-P. Ding and X.-F. Huang, *J. Phys. Chem. C*, 2013, **117**, 10643–10652.

67 M. Zhang, H. Yan, Q. Wei and H. Wang, *Comput. Mater. Sci.*, 2013, **68**, 371–378.

16970 | *Phys. Chem. Chem. Phys.*, 2024, **26**, 16963–16971

This journal is © the Owner Societies 2024

68 C. Ying, E. Zhao, L. Lin and Q. Hou, *Mod. Phys. Lett. B*, 2014, **28**, 1450213.

69 F.-G. Kuang, X.-Y. Kuang, S.-Y. Kang and X.-F. Huang, *Curr. Inorg. Chem.*, 2015, **5**, 143–150.

70 A. Van Der Geest and A. Kolmogorov, *CALPHAD: Comput. Coupling Phase Diagrams Thermochem.*, 2014, **46**, 184–204.

71 J. Wu and G. Yang, *Comput. Mater. Sci.*, 2014, **82**, 86–91.

72 G. Zhang, T. Bai, H. Yan and Y.-R. Zhao, *Chin. Phys. B*, 2015, **24**, 106104.

73 C. Ying, X. Bai, Y. Du, E. Zhao, L. Lin and Q. Hou, *Int. J. Mod. Phys. B*, 2016, **30**, 1650131.

74 X. Miao, W. Xing, F. Meng and R. Yu, *Solid State Commun.*, 2017, **252**, 40–45.

75 C. Ying, T. Liu, L. Lin, E. Zhao and Q. Hou, *Comput. Mater. Sci.*, 2018, **144**, 154–160.

76 H. Wu, Y. X. Wang, Z. Xin Yan, W. Liu, Z. Q. Wang and J. B. Gu, *Appl. Phys. A: Mater. Sci. Process.*, 2023, **129**, 175.

77 Y. Wang, J. Lv, L. Zhu and Y. Ma, *Comput. Phys. Commun.*, 2012, **183**, 2063–2070.

78 P. Giannozzi, S. Baroni, N. Bonini, M. Calandra, R. Car, C. Cavazzoni, D. Ceresoli, G. L. Chiarotti, M. Cococcioni and I. Dabo, *J. Phys.: Condens. Matter*, 2009, **21**, 395502.

79 M. Methfessel and A. Paxton, *Phys. Rev. B: Condens. Matter Mater. Phys.*, 1989, **40**, 3616.

80 S. Baroni, S. De Gironcoli, A. Dal Corso and P. Giannozzi, *Rev. Mod. Phys.*, 2001, **73**, 515.

81 P. B. Allen and R. C. Dynes, *Phys. Rev. B: Condens. Matter Mater. Phys.*, 1975, **12**, 905–922.

82 P. Morel and P. W. Anderson, *Phys. Rev.*, 1962, **125**, 1263–1271.

83 X.-Q. Chen, H. Niu, D. Li and Y. Li, *Intermetallics*, 2011, **19**, 1275–1281.

84 Y. Tian, B. Xu and Z. Zhao, *Int. J. Refract. Met. Hard Mater.*, 2012, **33**, 93–106.

85 Y. Kong, O. V. Dolgov, O. Jepsen and O. K. Andersen, *Phys. Rev. B: Condens. Matter Mater. Phys.*, 2001, **64**, 020501.

86 M. Aykol, S. S. Dwaraknath, W. Sun and K. A. Persson, *Sci. Adv.*, 2018, **4**, eaaq0148.

87 D. Zhou, D. V. Semenok, H. Xie, X. Huang, D. Duan, A. Aperis, P. M. Oppeneer, M. Galasso, A. I. Kartsev, A. G. Kvashnin, A. R. Oganov and T. Cui, *J. Am. Chem. Soc.*, 2020, **142**, 2803–2811.

88 Y. Quan, K.-W. Lee and W. E. Pickett, *Phys. Rev. B*, 2021, **104**, 224504.

89 H. J. Choi, D. Roundy, H. Sun, M. L. Cohen and S. G. Louie, *Nature*, 2002, **418**, 758–760.

90 A. Yang, X. Tao, Y. Quan and P. Zhang, *Phys. Rev. B*, 2023, **108**, 075203.

91 Y.-L. Han, Y.-P. Li, L. Yang, H.-D. Liu, N. Jiao, B.-T. Wang, H.-Y. Lu and P. Zhang, *Mater. Today Phys.*, 2023, **30**, 100954.

92 F. Mouhat and F. Coudert, *Phys. Rev. B: Condens. Matter Mater. Phys.*, 2014, **90**, 224104.

This journal is © the Owner Societies 2024

Phys. Chem. Chem. Phys., 2024, **26**, 16963–16971 | **16971**